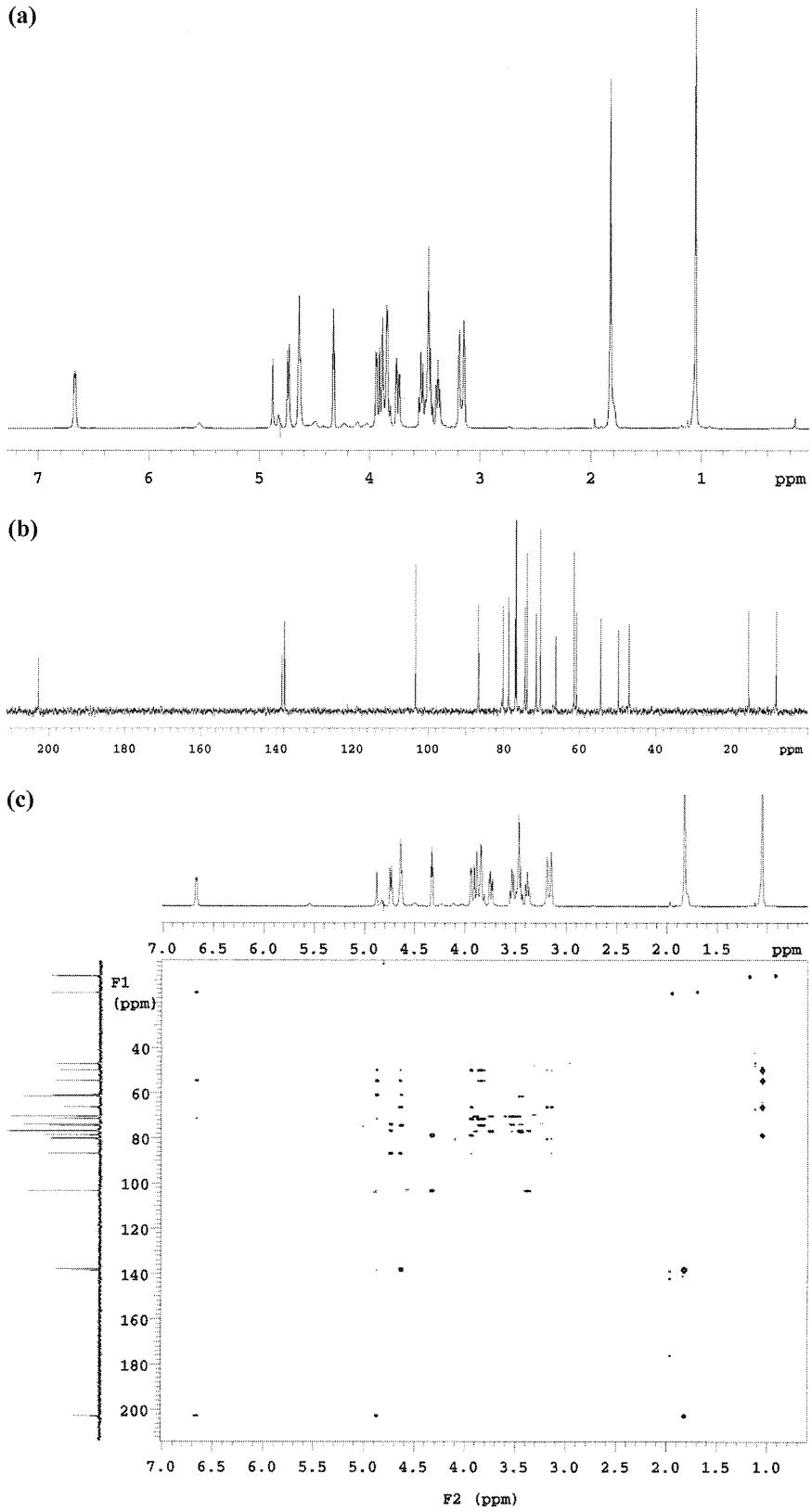

Figure 2. ^{1}H NMR spectrum (a), ^{13}C NMR spectrum (b), and HMBC spectrum (c) of nivalenol-3-*O*-*β*-D-glucopyranoside.

in nivalenol and 4 product ion spectra. From these results, 4 was suspected to be a nivalenol monoglycoside.

Isolation and Structure Determination of a Nivalenol Glycoside. Compound 4 was extracted from acetonitrile/water (85:15, v/v) from wheat. The extracts were fractionated by silica gel column chromatography, followed by liquid–liquid extraction. Further purification by C18 cartridges and reverse-phase HPLC afforded 4 in a yield of 9.2 mg from 12 kg of wheat. The ^{1}H and ^{13}C NMR spectra of 4 confirmed that it is a monoglycoside of nivalenol (Figure 2a,b). The sugar present in

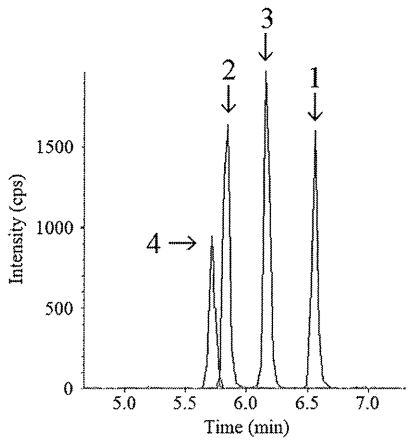

Figure 3. LC-MS/MS chromatogram of a standard solution (30 ng/mL concentrations of each analyte). Peaks: deoxynivalenol (**1**) (m/z 295 → 265); nivalenol (**2**) (m/z 371 → 281); deoxynivalenol-3-*O*-*β*-D-glucopyranoside (**3**) (m/z 517 → 427); nivalenol-3-*O*-*β*-D-glucopyranoside (**4**) (m/z 533 → 263).

4 was identified as glucose from NMR data, which are summarized in Table 1. A long-range coupling between C-3 of the nivalenol moiety and C-1′ of glucose observed in the HMBC spectrum of **4** showed that **4** was a nivalenol-3-*O*-glucopyranoside (Figure 2c). The $J_{H\text{-}1',H\text{-}2'}$ value (7.8 Hz) indicated a *β*-glycosidic linkage. Treating the acid hydrolysate of **4** with D-glucose oxidase showed the D configuration of the glucose residue of **4**. The structure of **4** was thus assigned as nivalenol-3-*O*-*β*-D-glucopyranoside (Figure 1).

Analytical Methods for Determination of Nivalenol, Deoxynivalenol, and Their Glucosides. Two purification methods were examined for the simultaneous determination of nivalenol, nivalenol-3-*O*-*β*-D-glucopyranoside, deoxynivalenol, and deoxynivalenol-3-*O*-*β*-D-glucopyranoside. The first is a method using a multifunctional column, InertSep VRA-3. The column, which contains ion exchange and reverse phase resins, is designed for purifying mycotoxins and agricultural chemicals from cereals. Previously, our group has reported a purification method using InertSep VRA-3 for the identification of deoxynivalenol, 3-acetyldeoxynivalenol, 15-acetyldeoxynivalenol, and deoxynivalenol-3-*O*-*β*-D-glucopyranoside in corn-based products.[25] The reported method was slightly modified to obtain good recoveries for nivalenol and nivalenol-3-*O*-*β*-D-glucopyranoside. The second is a method using a commercial immunoaffinity column. Some immunoaffinity columns that are designed for simultaneous purification of deoxynivalenol and nivalenol have recently been developed. In a preliminary study, deoxynivalenol, nivalenol, and their glucosides could be recovered from an immunoaffinity column, DON-NIV WB. Quantitation of the mycotoxins was performed by LC-MS/MS. A typical chromatogram is shown in Figure 3. To validate the two methods, they were applied to the analysis of spiked wheat samples containing nivalenol, nivalenol-3-*O*-*β*-D-glucopyranoside, deoxynivalenol, and deoxynivalenol-3-*O*-*β*-D-glucopyranoside at four levels in six replicates. Recoveries in the InertSep VRA-3 method were 81.5−91.3% for nivalenol, 69.8−75.3% for nivalenol-3-*O*-*β*-D-glucopyranoside, 65.8−71.7% for deoxynivalenol, and 68.3−85.3% for deoxynivalenol-3-*O*-*β*-D-glucopyranoside, whereas recoveries in the DON-NIV WB method were 87.1−93.3% for nivalenol, 94.1−103.5% for nivalenol-3-*O*-*β*-D-glucopyranoside, 86.4−96.5% for deoxynivalenol, and 95.0−100.1% for deoxynivalenol-3-*O*-*β*-D-glucopyranoside (Table 2). The LOQs for all analytes were within the range of 1−3 μg/kg. This result showed that both methods could be used to determine the four mycotoxins and that the recoveries obtained by the immunoaffinity column method were better than those obtained by the multifunctional column method.

The concentrations of nivalenol, nivalenol-3-*O*-*β*-D-glucopyranoside, deoxynivalenol, and deoxynivalenol-3-*O*-*β*-D-glucopyranoside in wheat samples were quantitated by the analytical method using an immunoaffinity column (Table 3). Nivalenol

Table 2. Limits of Quantitation (LOQ), Spiking Concentrations, and Recovery of Toxins for Validation of the Methods

			recovery (%)			
			InertSep VRA-3		DON-NIV WB	
analyte	LOQ (μg/kg)	spiking concn (μg/kg)	mean	RSD	mean	RSD
nivalenol	2	10	85.9	11.3	92.9	5.9
		50	85.3	3.1	93.3	3.2
		250	81.5	4.0	87.1	3.9
		1000	91.3	2.5	87.4	1.1
nivalenol-3-*O*-*β*-D-glucopyranoside	3	10	75.3	12.5	96.9	6.4
		50	73.6	4.9	103.1	5.5
		250	69.8	1.7	94.1	2.0
		1000	73.0	0.8	103.5	3.7
deoxynivalenol	2	10	71.1	9.0	94.8	12.0
		50	66.1	3.7	96.5	4.5
		250	65.8	3.0	86.4	1.0
		1000	71.7	1.2	88.6	4.4
deoxynivalenol-3-*O*-*β*-D-glucopyranoside	1	10	68.3	8.6	99.3	4.6
		50	77.2	5.8	100.1	4.3
		250	77.0	2.6	95.0	2.3
		1000	85.3	1.7	98.7	3.9

Table 3. Concentrations of Nivalenol, Nivalenol-3-*O*-*β*-D-glucopyranoside, Deoxynivalenol, and Deoxynivalenol-3-*O*-*β*-D-glucopyranoside in Wheat

wheat no.	nivalenol (mg/kg)	nivalenol-3-*O*-*β*-D-glucopyranoside (mg/kg)	nivalenol-3-*O*-*β*-D-glucopyranoside/nivalenol (mol %)	deoxynivalenol (mg/kg)	deoxynivalenol-3-*O*-*β*-D-glucopyranoside (mg/kg)	deoxynivalenol-3-*O*-*β*-D-glucopyranoside/deoxynivalenol (mol %)
1	0.37	0.15	27	10	1.5	10
2	0.54	0.22	27	0.67	0.15	14
3	1.5	0.54	24	3.6	0.27	5
4	1.7	0.30	12	5.6	0.62	7
5	15	4.0	18	0.23	0.05	14

and nivalenol-3-*O*-*β*-D-glucopyranoside were detected in all samples, and the percentages of nivalenol-3-*O*-*β*-D-glucopyranoside to nivalenol ranged from 12 to 27%. Deoxynivalenol and deoxynivalenol-3-*O*-*β*-D-glucopyranoside were also found in the samples, and the percentage of deoxynivalenol-3-*O*-*β*-D-glucopyranoside to deoxynivalenol was within the range of 5−14%.

In this study, a new derivative of nivalenol was isolated from nivalenol-contaminated wheat and was identified as nivalenol-3-*O*-*β*-D-glucopyranoside. Methods for the simultaneous determination of nivalenol, deoxynivalenol, and their glucosides in wheat were successfully developed and validated. Co-contamination of nivalenol-3-*O*-*β*-D-glucopyranoside with nivalenol, deoxynivalenol, and deoxynivalenol-3-*O*-*β*-D-glucopyranoside was observed in wheat, and the ratio of nivalenol-3-*O*-*β*-D-glucopyranoside to nivalenol was equivalent to that of deoxynivalenol-3-*O*-*β*-D-glucopyranoside to deoxynivalenol reported previously.[17] Because glycosylation is considered to be a detoxification process, it seems likely that nivalenol-3-*O*-*β*-D-glucopyranoside shows lower toxicity than nivalenol. However, as with deoxynivalenol-3-*O*-*β*-D-glucopyranoside, nivalenol-3-*O*-*β*-D-glucopyranoside may be hydrolyzed by intestinal bacteria and toxic nivalenol may be produced in the body. Therefore, nivalenol-3-*O*-*β*-D-glucopyranoside can be an important contributor to dietary exposure to trichothecene mycotoxins and should be monitored together with nivalenol, deoxynivalenol, and deoxynivalenol-3-*O*-*β*-D-glucopyranoside in foodstuffs.

■ ASSOCIATED CONTENT

Supporting Information

HPLC chromatograms of the three steps of purification of nivalenol-3-*O*-*β*-D-glucopyranoside. This material is available free of charge via the Internet at http://pubs.acs.org.

■ AUTHOR INFORMATION

Corresponding Author

*(T.Y.) Phone: +81-3-3700-1141. Fax: +81-3-3700-9852. E-mail: t-yoshinari@nihs.go.jp.

Funding

This study was funded by The Tojuro Iijima Foundation for Food Science and Technology.

Notes

The authors declare no competing financial interest.

■ ACKNOWLEDGMENTS

We thank Dr. T. Nakajima (Ministry of Agriculture, Forestry and Fisheries) for donating wheat samples.

■ REFERENCES

(1) McCormick, S. P.; Stanley, A. M.; Stover, N. A.; Alexander, N. J. Trichothecenes: from simple to complex mycotoxins. *Toxins* **2011**, *3*, 802−814.

(2) Tanaka, T.; Sugiura, Y. Levels and pattern of contamination with trichothecenes in cereal grains and their risk assessment. *JSM Mycotoxins* **2003**, *53*, 119−121.

(3) Schollenberger, M.; Müller, H. M.; Rüfle, M.; Suchy, S.; Plank, S.; Drochner, W. Natural occurrence of 16 *Fusarium* toxins in grains and feedstuffs of plant origin from Germany. *Mycopathologia* **2006**, *161*, 43−52.

(4) Scudamore, K. A.; Patel, S. Occurrence of *Fusarium* mycotoxins in maize imported into the UK, 2004−2007. *Food Addit. Contam. A* **2009**, *26*, 363−371.

(5) Kubosaki, A.; Aihara, M.; Park, B. J.; Sugiura, Y.; Shibutani, M.; Hirose, M.; Suzuki, Y.; Takatori, K.; Sugita-Konishi, Y. Immunotoxicity of nivalenol after subchronic dietary exposure to rats. *Food Chem. Toxicol.* **2008**, *46*, 253−258.

(6) Takahashi, M.; Shibutani, M.; Sugita-Konishi, Y.; Aihara, M.; Inoue, K.; Woo, G. H.; Fujimoto, H.; Hirose, M. A 90-day subchronic toxicity study of nivalenol, a trichothecene mycotoxin, in F344 rats. *Food Chem. Toxicol.* **2008**, *46*, 125−135.

(7) Sobrova, P.; Adam, V.; Vasatkova, A.; Beklova, M.; Zeman, L.; Kizek, R. Deoxynivalenol and its toxicity. *Interdiscip. Toxicol.* **2010**, *3*, 94−99.

(8) Peraica, M.; Radić, B.; Lucić, A.; Pavlović, M. Toxic effects of mycotoxins in humans. *Bull. WHO* **1999**, *77*, 754−766.

(9) Food Safety Commission of Japan. Risk assessment report deoxynivalenol and nivalenol (mycotoxin); available online at http://www.fsc.go.jp/english/evaluationreports/nm_toxins/rar_donniv_fs872_2010_nm.pdf (accessed Oct 1, 2013).

(10) European Food Safety Authority. Scientific opinion on risks for animal and public health related to the presence of nivalenol in food and feed. *EFSA J.* **2013**, *11*, 3262.

(11) Berthiller, F.; Crews, C.; Dall'Asta, C.; Saeger, S. D.; Haesaert, G.; Karlovsky, P.; Oswald, I. P.; Seefelder, W.; Speijers, G.; Stroka, J. Masked mycotoxins: a review. *Mol. Nutr. Food Res.* **2013**, *57*, 165−186.

(12) Berthiller, F.; Dall'Asta, C.; Schuhmacher, R.; Lemmens, M.; Adam, G.; Krska, R. Masked mycotoxins: determination of a deoxynivalenol glucoside in artificially and naturally contaminated wheat by liquid chromatography-tandem mass spectrometry. *J. Agric. Food Chem.* **2005**, *53*, 3421−3425.

(13) Miller, J. D.; Young, J. C. Deoxynivalenol in an experimental *Fusarium graminearum* infection of wheat. *Can. J. Plant Pathol.* **1985**, *7*, 132−134.

(14) Boutigny, A. L.; Richard, F. F.; Barreau, C. Natural mechanisms for cereal resistance to the accumulation of *Fusarium* trichothecenes. *Eur. J. Plant Pathol.* **2008**, *121*, 411−423.

(15) Poppenberger, B.; Berthiller, F.; Lucyshyn, D.; Sieberer, T.; Schuhmacher, R.; Krska, R.; Kuchler, K.; Glössl, J.; Luschnig, C.; Adam, G. Detoxification of the *Fusarium* mycotoxin deoxynivalenol by a UDP-glucosyltransferase from *Arabidopsis thaliana*. *J. Biol. Chem.* **2003**, *278*, 47905−47914.

(16) WHO. *Evaluation of Certain Contaminants in Food*; WHO Technical Report Series 959; WHO: Rome, Italy, 2010; pp 37−48.

(17) Berthiller, F.; Dall'Asta, C.; Corradini, R.; Marchelli, R.; Sulyok, M.; Krska, R.; Adam, G.; Schuhmacher, R. Occurrence of deoxynivalenol and its 3-β-D-glucoside in wheat and maize. *Food Addit. Contam. A* **2009**, *26*, 507−511.
(18) Rasmussen, P. H.; Nielsen, K. F.; Ghorbani, F.; Spliid, N. H.; Nielsen, G. C.; Jørgensen, L. N. Occurrence of different trichothecenes and deoxynivalenol-3-β-D-glucoside in naturally and artificially contaminated Danish cereal grains and whole maize plants. *Mycotoxin Res.* **2012**, *28*, 181−190.
(19) Varga, E.; Malachova, A.; Schwartz, H.; Krska, R.; Berthiller, F. Survey of deoxynivalenol and its conjugates deoxynivalenol-3-glucoside and 3-acetyl-deoxynivalenol in 374 beer samples. *Food Addit. Contam. A* **2013**, *30*, 137−146.
(20) Berthiller, F.; Krska, R.; Domig, K. J.; Kneifel, W.; Juge, N.; Schuhmacher, R.; Adam, G. Hydrolytic fate of deoxynivalenol-3-glucoside during digestion. *Toxicol. Lett.* **2011**, *206*, 264−267.
(21) Gratz, S. W.; Duncan, G.; Richardson, A. J. The human fecal microbiota metabolizes deoxynivalenol and deoxynivalenol-3-glucoside and may be responsible for urinary deepoxy-deoxynivalenol. *Appl. Environ. Microbiol.* **2013**, *79*, 1821−1825.
(22) Nakagawa, H.; Ohmichi, K.; Sakamoto, S.; Sago, Y.; Kushiro, M.; Nagashima, H.; Yoshida, M.; Nakajima, T. Detection of a new *Fusarium* masked mycotoxin in wheat grain by high-resolution LC-Orbitrap MS. *Food Addit. Contam. A* **2011**, *28*, 1447−1456.
(23) Busman, M.; Poling, S. M.; Maragos, C. M. Observation of T-2 toxin and HT-2 toxin glucosides from *Fusarium sporotrichioides* by liquid chromatography coupled to tandem mass spectrometry (LC-MS/MS). *Toxins* **2011**, *3*, 1554−1568.
(24) Lattanzio, V. M.; Visconti, A.; Haidukowski, M.; Pascale, M. Identification and characterization of new *Fusarium* masked mycotoxins, T2 and HT2 glycosyl derivatives, in naturally contaminated wheat and oats by liquid chromatography-high-resolution mass spectrometry. *J. Mass Spectrom.* **2012**, *47*, 466−475.
(25) Yoshinari, T.; Ohnishi, T.; Kadota, T.; Sugita-Konishi, Y. Development of a purification method for simultaneous determination of deoxynivalenol and its acetylated and glycosylated derivatives in corn grits and corn flour by liquid chromatography-tandem mass spectrometry. *J. Food Prot.* **2012**, *75*, 1355−1358.

Analytica Chimica Acta 888 (2015) 126–130

Contents lists available at ScienceDirect

Analytica Chimica Acta

journal homepage: www.elsevier.com/locate/aca

Development of a rapid method for the quantitative determination of deoxynivalenol using Quenchbody

Tomoya Yoshinari [a], Hiroyuki Ohashi [b], Ryoji Abe [b], Rena Kaigome [b], Hideo Ohkawa [c], Yoshiko Sugita-Konishi [d, *]

[a] Division of Microbiology, National Institute of Health Sciences, 1-18-1, Kamiyoga, Setagaya-ku, Tokyo 158-8501, Japan
[b] Biomedical Division, Ushio Inc., 1-12 Minamiwatarida-cho, Kawasaki-ku, Kawasaki 210-0855, Japan
[c] Research Center for Environmental Genomics, Kobe University, 1-1 Rokkodai, Nada, Kobe 657-8501, Japan
[d] Department of Food and Life Science, Azabu University, 1-17-71 Fuchinobe, Chuo-ku, Sagamihara, Kanagawa 252-5201, Japan

HIGHLIGHTS

- A rapid method for quantitation of DON using Q-body has been developed.
- A recovery test using the anti-DON Q-body was performed.
- The concentrations of DON in wheat were quantitated by the anti-DON Q-body.

GRAPHICAL ABSTRACT

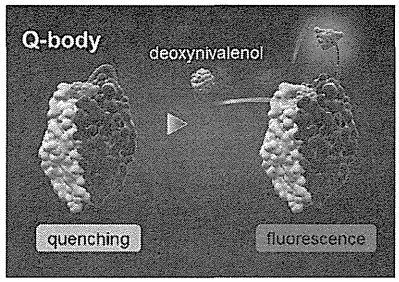

ARTICLE INFO

Article history:
Received 28 February 2015
Received in revised form
30 June 2015
Accepted 3 July 2015
Available online 8 August 2015

Keywords:
Deoxynivalenol
Wheat
Quenchbody
Rapid analysis technique

ABSTRACT

Quenchbody (Q-body) is a novel fluorescent biosensor based on the antigen-dependent removal of a quenching effect on a fluorophore attached to antibody domains. In order to develop a method using Q-body for the quantitative determination of deoxynivalenol (DON), a trichothecene mycotoxin produced by some *Fusarium* species, anti-DON Q-body was synthesized from the sequence information of a monoclonal antibody specific to DON. When the purified anti-DON Q-body was mixed with DON, a dose-dependent increase in the fluorescence intensity was observed and the detection range was between 0.0003 and 3 mg L^{-1}. The coefficients of variation were 7.9% at 0.003 mg L^{-1}, 5.0% at 0.03 mg L^{-1} and 13.7% at 0.3 mg L^{-1}, respectively. The limit of detection was 0.006 mg L^{-1} for DON in wheat. The Q-body showed an antigen-dependent fluorescence enhancement even in the presence of wheat extracts. To validate the analytical method using Q-body, a spike-and-recovery experiment was performed using four spiked wheat samples. The recoveries were in the range of 94.9–100.2%. The concentrations of DON in twenty-one naturally contaminated wheat samples were quantitated by the Q-body method, LC-MS/MS and an immunochromatographic assay kit. The LC-MS/MS analysis showed that the levels of DON contamination in the samples were between 0.001 and 2.68 mg kg^{-1}. The concentrations of DON quantitated by LC-MS/MS were more strongly correlated with those using the Q-body method ($R^2 = 0.9760$) than the immunochromatographic assay kit ($R^2 = 0.8824$). These data indicate that the Q-body system for the determination of DON in wheat samples was successfully developed and Q-body is expected to have a range of applications in the field of food safety.

* Corresponding author.
E-mail address: y-konishi@azabu-u.ac.jp (Y. Sugita-Konishi).

http://dx.doi.org/10.1016/j.aca.2015.07.020
0003-2670/

1. Introduction

Deoxynivalenol (DON) is a trichothecene mycotoxin produced by some species of *Fusarium*, such as *Fusarium graminearum* and *Fusarium culmorum*. Because these fungi have a large geographical distribution, contamination of DON in agricultural products, including wheat, barley and maize, has occurred worldwide [1–4]. The studies about the toxicity of DON using experimental animals has showed that DON causes vomiting, the loss of appetite, lower body weight gains and immunosuppression [5,6]. Some epidemiological studies indicate that human exposure to DON induces acute symptoms, such as diarrhea, headache, nausea and vomiting. Outbreaks of mycotoxicoses associated with the consumption of cereals contaminated with trichothecenes have been reported in Asian countries [7]. In order to prevent the intake of DON, regulatory or guideline limits for DON in food have been set in some counties in the late 1990s. Japan has set a provisional regulatory limit of 1.1 mg kg^{-1} of DON for wheat in 2002. In the EU, the maximum limits are set between 200 μg kg^{-1} for processed cereal-based foods and baby foods for infants and young children and 1750 μg kg^{-1} for unprocessed durum wheat, oats and maize, while the USA has proposed a guidance level of 1000 μg kg^{-1} for DON in final wheat products [8].

Many analytical methods for the determination of DON in cereals have been developed. In order to quantitate a small amount of DON accurately, instrumental analytical techniques using HPLC, GC–MS, LC–MS or LC–MS/MS have been recently reported [9–12]. A method using a multifunctional clean-up column coupled with HPLC has been validated by an interlaboratory study and is used as the official analytical method for the determination of DON contamination in wheat in Japan [13]. An HPLC method with immunoaffinity column cleanup and UV detection for determination of DON in cereal and cereal products has been adopted by the European Committee for Standardization (EN 15891:2010). For rapid screening of DON contamination in food, several methods based on immunochromatographic (IC) assay, enzyme-linked immunosorbent assay (ELISA), a surface plasmon resonance immunoassay and a fluorescence polarization immunoassay have been developed [14–19]. Some analytical kits based on IC assay and ELISA for DON detection in cereals are commercially available. In Japan, ELISA has been adopted as an official method for screening of DON in wheat. In the case that the measured value by ELISA is above the cut-off value, 0.7 mg kg^{-1}, the concentration of DON in the sample is required to be quantitated by the official instrumental method. It is recommended to take technical training before using the ELISA kit because experience is essential for accurate and reliable testing. Therefore, in order to perform more efficient screening of DON in foods, development of a method which enables rapid quantitation of DON without requiring a specific skill is needed.

Quenchbody (Q-body) is a novel fluorescent biosensor based on the antigen-dependent removal of a quenching effect on a fluorophore attached to antibody domains [20–22]. In the absence of a target molecule of Q-body, the fluorescence of Q-body is quenched by the interaction between a fluorophore and conserved tryptophan residues in antibody variable region, whereas, in the presence of a target molecule, a conformational change of Q-body by antigen–antibody interaction causes fluorescence emission from the unquenched fluorophore. This reaction occurs just after mixing Q-body and antigen, and the result can be obtained only by measuring the fluorescence without some time-consuming steps, such as washing and soaking. By designing the antigen biding site in Q-body, detection systems targeting a variety of compounds have been developed until now. For example, bisphenol A, osteocalcin and some drugs, such as morphine and cocaine, have been successfully quantified by using Q-body system [20].

The aim of this study was to develop a rapid method for quantitation of DON using Q-body. Q-body for analysis of DON was designed from sequence information of a monoclonal antibody specific to DON, and a recovery test using spiked wheat samples was performed in order to validate the analytical method using the Q-body. The concentrations of DON in naturally contaminated wheat samples were quantitated by three different methods, the Q-body system, IC assay kit and LC-MS/MS, and the usefulness of the Q-body system was evaluated by comparing the results.

2. Materials and methods

2.1. Materials

The stock solution of DON (100 mg L^{-1}) was prepared by dissolving crystalline DON (Sigma–Aldrich, St. Louis, MO, USA) in distilled water. The stock solution was diluted with distilled water to make the standard solutions of DON. LC/MS-grade acetonitrile and water were purchased from Wako Pure Chemical Industries, Ltd. (Osaka, Japan). The naturally contaminated wheat samples were imported from USA, Australia or Canada. They were supplied by an import inspection agency in 2012 and 2013.

2.2. Vector construction

Vectors for anti-DON Q-body expression were constructed according to a previous report [21]. The details are as follows. The PCR primers used in this study are shown in Supplementary Material 1. An expression vector pROX-DON-VH-CH1, harboring a T7 promoter-controlled heavy-chain Fd (VH–CH1) gene of anti-DON antibody [23] fused with an N-terminal ProX tag and a C-terminal FLAG tag, was generated by splice-overlap-extension (SOE) PCR. The VH chain was combined by SOE PCR with specific primers (Don-H-P1, Don-H-P2, Don-H-P3, Don-H-T1, Don-H-T2, Don-H-T3, Don-H-P and Don-H-T). CH1 was amplified using CH1–P and CH1-FLAG-T from a vector, pCHCκ, harboring the mouse IgG1 CH1 gene and Cκ gene. pCHCκ was prepared by an artificial gene synthesis service (Funakoshi, Japan). The vector has the CH1 and Cκ sequences, AKTTPPSVYPLAPGSAAQTNSMVTLGCLVKGYFPEPVTVT WNSGSLSSGVHTFPAVLESDLYTLSSSVTVPSSPRPSETVTCNVAHPASST KVDKKIVPRDC and ADAAPTVSIFPPSSEQLTSGGASVVCFLNNFYPK-DINVKWKIDGSERQNGVLNSWTDQDSKDSTYSMSSTLTLTKDEYERHN SYTCEATHKTSTSPIVKSFNRNEC. The amplified VH and CH1 genes were linked by SOEPCR with 5′ GS-primer and CH1-FLAG-T, and the construct was cloned into the NcoI- and BamHI-digested pROX-FL92 (ProteinExpress, Chiba, Japan) using the In-Fusion PCR cloning kit (Clontech, USA). In addition, an expression vector pROX-DON-VL-Cκ harboring a T7 promoter-controlled light-chain (VL-Cκ) gene of anti-DON antibody fused with an N-terminal ProX tag containing an amber codon (ATG TCT AAA CAA ATC GAA GTA AAC TAG TCT AAT GAG) and a C-terminal His tag was constructed by SOE PCR. The VL chain was combined by SOE PCR with primers (Don-L-P1, Don-L-P2, Don-L-P3, Don-L-T1, Don-L-T2, Don-L-T3, Don-L-P and Don-L-T). The mouse Cκ gene was amplified using the 5′-primer (Cκ Pv3) and 3′-primer (Cκ+C-His_T) from pCHCκ. The amplified VL and Cκ genes were linked by SOE PCR using 5′ 2 GS-primer and Cκ+C-His_T, and the construct was then cloned into NcoI- and SmaI-digested pROX-FL92 using the In-Fusion PCR cloning kit.

2.3. Cell-free co-transcription/translation

Cell-free co-transcription/translation and purification to obtain the anti-DON Q-body solution were conducted as previously described [21]. TAMRA-C6-tRNA was synthesized as previously described [20]. The incorporation of TAMRA-C6-AF into the N-

terminal region of Fab was performed using a cell-free transcription/translation system. The reaction mixture (60 μL) consisted of 41.1 μL of the reaction mix, 4.5 μL of amino acid mix, 0.4 μL of 120 mM glutathione (GSSG/GSH = 10/1), 4 μL of distilled water, 4 μL of plasmid DNAs (50 ng μL^{-1}) and 6 μL of aminoacyl-tRNA (1440 pmol). All the reagents used, with the exception of the plasmid and tRNA, were provided in Musaibou-kun kit (Taiyo Nippon Sanso Corporation, Japan). The reaction mixture was incubated at 37 °C for 2 h and subsequently incubated at 4 °C for 16 h. Tandem affinity purification with anti-Flag- and nickel-affinity chromatography was then performed. First, the reaction mixture (60 μL) was incubated with 20 μL of Flag M2 affinity gel. After incubation at room temperature for 15 min, the column was washed three times with wash buffer (20 mM phosphate, 0.5 M NaCl, 0.1% polyoxyethylene lauryl ether, pH 7.4). The bound proteins were subsequently eluted with two 200-μL volumes of wash buffer containing 100 μg mL^{-1} of Flag peptide. The eluted proteins were then applied to a His Spin Trap Column (GE Healthcare, Piscataway, NJ, USA). After incubation at room temperature for 15 min, the column was washed three times with wash buffer containing 60 mM imidazole. The bound proteins were then eluted with two 200-μL volumes of wash buffer containing 0.5 M imidazole. The eluate was subsequently passed through an UltraFree-0.5 centrifugal device (Millipore, Billerica, MA) and equilibrated with phosphate buffered saline supplemented with Tween-20 (PBST, 10 mM phosphate, 137 mM NaCl, 2.7 mM KCl, 0.05% Tween 20, pH 7.4) to concentrate the protein in the buffer. The concentration of the labeled Fab protein was determined by comparing the fluorescence intensities of a known concentration of free TAMRA dye (Anaspec, Fremont, CA) and the sample under denaturing conditions in 7 M GdnHCl, 100 mM DTT, pH 7.4.

2.4. Quantitation of DON by the Q-body method

The purified anti-DON Q-body (16 nM, 30 μL) in PBST containing 0.2% BSA was mixed with 30 μL of the standard solution of DON, and the fluorescence intensity was measured at 580 nm with excitation set at 530 nm on a SpectraMax Paradigm Multi-Mode reader (Molecular Devices, USA). The EC_{50} values were calculated using curve fitting of the observed fluorescence intensities at the maximum emission wavelength and employing a sigmoidal dose–response model based on the ImageJ software (http://rsbweb.nih.gov/ij/). All the fluorescence intensities were normalized by setting the intensity of each sample at the zero dose (without antigen) as one, at the maximum emission wavelength, unless otherwise stated. The limit of detection was assessed by analyzing a blank sample 6 times and calculating the 3.3 SD (standard deviation) limit. For the quantitation of DON in wheat, 10 g of the wheat sample was extracted with 40 mL of distilled water and then shaken for 10 min. After centrifugation (12,000 *g*, 10 min), the supernatant was diluted four times by distilled water and 30 μL of the dilution was mixed with the purified anti-DON Q-body (16 nM, 30 μL) in PBST containing 0.2% BSA, and the fluorescence intensity was measured. The water extract from wheat was prepared from DON-negative wheat (batch number: D-W-100; Trilogy Analytical Laboratory Inc., Washington, MO, USA). For the spike-and-recovery experiment, the DON-negative wheat was spiked at four concentrations (0.5, 1.0 2.0, and 5.0 mg kg^{-1}). The concentration of DON in wheat was calculated from a calibration curve, which was created by plotting the fluorescence intensity of eight standard solutions at different concentrations (0.0001, 0.0003, 0.001, 0.003, 0.01, 0.03, 0.1, 0.3, 1.0 and 3.0 mg L^{-1} final concentrations).

2.5. LC-MS/MS analytical method

The LC-MS/MS method was developed and validated in our previous study [24]. Twenty-five grams of the wheat sample was extracted with 100 mL of distilled water and then shaken for 30 min. After centrifugation (3000 *g*, 10 min), the supernatant was collected. Aliquots of 10 mL of the supernatant were diluted with 50 mL of phosphate-buffered saline (PBS). After the diluted extract was filtered through a glass fiber filter GA-55 (Toyo Roshi Kaisha, Japan), 6 mL of the filtrate was applied to a DON-NIV WB immunoaffinity column (VICAM, Milford, MA, USA). The column was washed with 10 mL of PBS followed by a wash with 10 mL of distilled water. Toxins were eluted using 0.5 mL of methanol followed by 1.5 mL of acetonitrile. The eluate was dried under nitrogen at 40 °C. The residue was dissolved in 0.25 mL of 10% acetonitrile in water. LC-MS/MS analyses were performed with a 3200 Q TRAP LC-MS/MS system (AB Sciex, Foster City, CA, USA) equipped with an ESI source and an LC-20A series high performance LC system (Shimadzu Corp., Kyoto, Japan). The column used was a 150 mm × 2.1 mm i.d., 3 μm, Inertsil ODS-3 (GL Sciences, Inc., Tokyo, Japan). Chromatographic separation was achieved at 40 °C using a gradient elution of 5–73% acetonitrile in water from 0 to 8 min and followed by an isocratic elution of 90% acetonitrile in water from 8 to 10 min at a flow rate of 0.2 mL min^{-1}. The ESI source was operated at 400 °C in the negative ionization mode. The following multiple reaction monitoring transitions were used: DON, 295 $[M - H]^-$ to 265 (quantifier ion: collision energy, −12 eV) and 138 (qualifier ion: collision energy, −28 eV). The other conditions were described in our previous report [24].

2.6. Immunochromatographic assay

The DON-V kit (VICAM) was used for the immunochromatographic (IC) assay. The assay was performed according to the manufacturer's protocol. The extraction was performed similarly to the Q-body method. Aliquots of 100 μL of the extract were diluted with 1.0 mL of distilled water. One hundred microliters of the diluted solution was mixed with 100 μL of the provided diluent, and 100 μL of the mixture was applied to the DON-V test strip. The strip was incubated at 25 °C for 3 min, and the signal was quantitated by a Vertu Lateral Flow Reader (VICAM).

3. Results and discussion

In order to confirm the antigen-dependent fluorescence enhancement of the synthesized Q-body for DON, the Q-body was mixed with the standard solutions of DON (0.0001, 0.0003, 0.001, 0.003, 0.01, 0.03, 0.1, 0.3, 1.0 and 3.0 mg L^{-1} final concentrations) and the fluorescence emission was measured (Fig. 1). The fluorescence intensities increased dose-dependently at the concentrations between 0.0003 and 3 mg L^{-1}. The relative 3.9-fold intensity was reached at a concentration of 3 mg L^{-1}, as compared with the basal intensity without DON, and the EC_{50} value was 0.03 mg L^{-1}. The coefficients of variation were 7.9% at 0.003 mg L^{-1}, 5.9% at 0.03 mg L^{-1} and 13.1% at 0.3 mg L^{-1}, respectively. The limit of detection was 0.006 mg kg^{-1} for DON in wheat. The concentration of DON in the wheat sample is 32-fold of the measured value because 10 g of the wheat sample was extracted with 40 mL of distilled water and the extract was diluted four times and the dilution was mixed with equal volume of the Q-body solution. The influence of the wheat matrix on the fluorescence increase was evaluated by mixing the Q-body and DON with or without the water extracted from the wheat. A dose-dependent increase of the fluorescence intensity was observed under both conditions (Supplementary Material 2). The water extracted from wheat significantly decreased the fluorescence increase of the Q-body, but the decreasing rate of the intensity was less than 1%. In order to evaluate cross-reactivity of the anti-DON Q-body against other

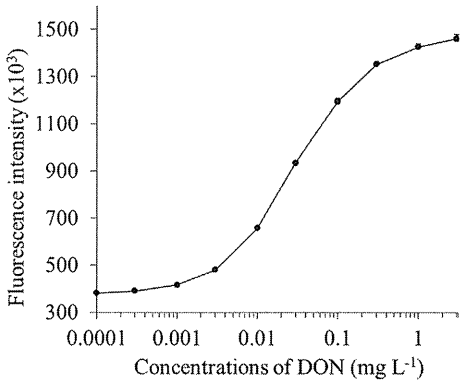

Fig. 1. The dose-dependent fluorescence enhancement of anti-DON Q-body. The standard solutions of DON were mixed with anti-DON Q-body and the fluorescence intensities were measured. Data are presented as the mean ± SD (n = 6).

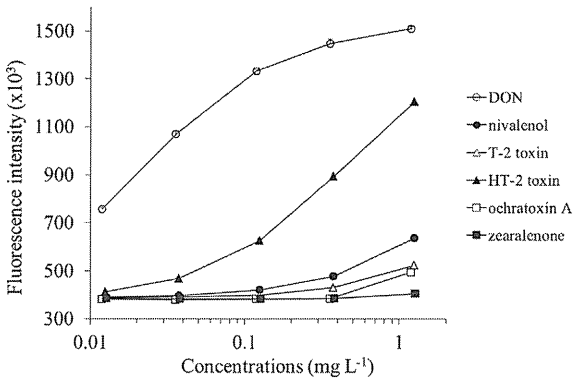

Fig. 2. Evaluation of cross-reactivity of anti-DON Q-body against mycotoxins occurring in wheat. The standard solutions of DON (○), nivalenol (●), T-2 toxin (△), HT-2 toxin (▲), ochratoxin A (□) or zearalenone (■) were mixed with anti-DON Q-body and the fluorescence intensities were measured (n = 3).

mycotoxins in wheat, the Q-body was mixed with nivalenol, T-2 toxin, HT-2 toxin, ochratoxin A or zearalenone and the fluorescence emission was measured (Fig. 2). The Q-body was most specific for DON (EC_{50} 0.03 mg L^{-1}) followed by HT-2 toxin (EC_{50} 0.55 mg L^{-1}). The EC_{50} values of other compounds were more than 1 mg L^{-1}. These results indicated that the Q-body method for DON was successfully constructed and can be used for the quantitation of DON. Because the wheat matrix hardly affected the fluorescence increase of the Q-body, purification steps were considered to be unnecessary for the determination of DON in wheat by the Q-body.

An analysis of the blank wheat sample and the spiked samples containing DON at four concentrations (0.5, 1.0 2.0, 5.0 mg kg^{-1}) in six replicates was performed to validate the method using Q-body. DON was extracted from the samples by water. The extract was diluted by distilled water and the dilution was mixed with Q-body and the emitted fluorescence was measured. The concentrations of DON in the samples were calculated by comparing the fluorescence intensity of the samples with that of the standard solutions. The calculated recoveries are shown in Table 1. The recoveries from the spiked samples were in the range of 94.9–100.2%. When the concentrations of DON in the spiked samples were quantitated by an IC kit, the recoveries were between 75.7 and 89.1%. This result showed that the Q-body could be used for the quantification of DON in wheat without any purification steps, and had the same capabilities at a commercially available IC kit.

Table 2
DON concentrations (mg kg^{-1}) in naturally contaminated wheat samples measured by LC-MS/MS, the Q-body system and an immunochromatographic kit.

Sample	LC-MS/MS		Q-body		IC kit	
	Conc.	p or n[a]	Conc.	p or n	Conc.	p or n
1	0.001	n	<0.007	n	<0.25	n
2	0.002	n	0.01	n	<0.25	n
3	0.07	n	0.05	n	<0.25	n
4	0.09	n	0.07	n	<0.25	n
5	0.23	n	0.19	n	<0.25	n
6	0.28	n	0.24	n	<0.25	n
7	0.29	n	0.30	n	<0.25	n
8	0.38	n	0.33	n	0.28	n
9	0.46	n	0.37	n	0.45	n
10	0.46	n	0.39	n	0.28	n
11	0.51	n	0.42	n	0.37	n
12	0.52	n	0.41	n	0.26	n
13	0.65	n	0.48	n	0.37	n
14	0.70	n	0.62	n	0.45	n
15	0.77	p	0.72	p	0.52	n
16	0.82	p	0.77	p	0.71	p
17	0.88	p	0.76	p	0.75	p
18	0.90	p	0.81	p	0.66	n
19	1.84	p	1.59	p	1.26	p
20	1.90	p	1.74	p	1.49	p
21	2.68	p	1.92	p	3.55	p

Abbreviation: IC, immunochromatographic; Conc., concentration.
[a] "p" means positive (more than 0.70 mg kg^{-1}) and "n" means negative (equal to or less than 0.70 mg kg^{-1}).

The DON concentrations in the naturally contaminated wheat samples were quantitated by three methods, LC-MS/MS, the Q-body assay system and the IC assay kit for the comparison of the analytical methods (Table 2). The values greater than 0.7 mg kg^{-1}, a cut-off value for the screening of DON in Japan, were considered to be positive (p) and those equal to or less than 0.7 mg kg^{-1} were regarded as negative (n). Fourteen samples (No. 1–14) were negative and 7 samples (No. 15–21) were positive in the both LC-MS/MS and the Q-body assay system, and the concordance rate of the results between the two methods was 100%. On the other hand, the concordance rate of the results between the LC-MS/MS analysis and the IC assay kit was 90%. The values measured by LC-MS/MS and the Q-body assay system or the IC assay kit were plotted (Fig. 3a and b). The concentrations of DON quantitated by LC-MS/MS were more strongly correlated with those using the Q-body assay system (R^2 = 0.9760) than the IC assay kit (R^2 = 0.8824). These results suggested that the Q-body assay system for DON has an equivalent performance to the widely used, commercially available IC assay kit.

Table 1
Spiking concentrations and the recovery of DON for validation of the methods.

Spiking conc. (μg kg^{-1})	Recovery (%)			
	Q-body		Immunochromatographic assay	
	Mean	RSD	Mean	RSD
500	96.1	1.5	82.3	19.2
1000	94.9	1.3	75.7	12.5
2000	100.2	3.8	86.4	6.9
5000	98.3	2.8	89.1	8.9

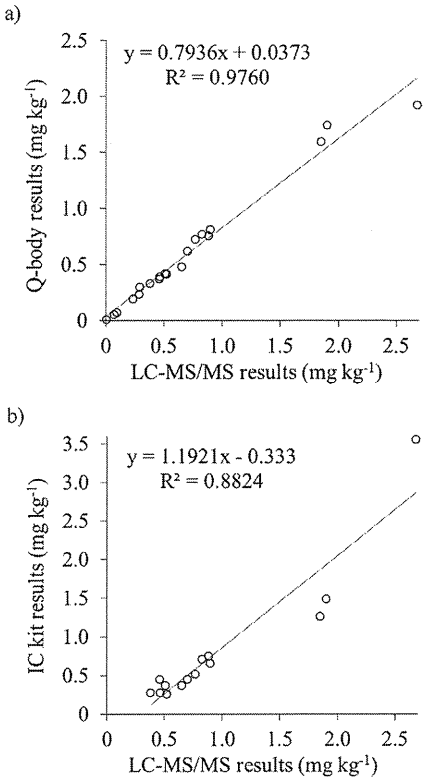

Fig. 3. Comparison of the concentrations of DON in the naturally contaminated wheat samples using LC-MS/MS and the Q-body assay system (a) or an immunochromatographic (IC) kit (b).

4. Conclusion

The results of a spike-and-recovery experiment and the comparison of the quantitative values of DON in the wheat samples indicate that the Q-body assay system has an adequate capacity to determine DON levels in wheat. This assay system is easier to use than the IC assay and ELISA kits, thus making it possible to perform rapid measurements. DON contaminates various types of foods and feedstuffs. In order to prove its practicality, whether the Q-body assay system is also applicable to other samples in addition to wheat is now being evaluated. Contamination with not only DON, but also various toxic compounds in foods is a significant concern from the viewpoint of food safety, and the development of easy and rapid methods for detecting contaminants in foods can contribute to alleviating the problem of food poisoning. Because the Q-body assay system can target a wide variety of compounds by simply altering the antigen binding, this system is therefore expected to have a wide range of applications in the field of food safety.

Appendix A. Supplementary data

Supplementary data related to this article can be found at http://dx.doi.org/10.1016/j.aca.2015.07.020.

References

[1] R.A. Canady, R.D. Coker, S.K. Egan, R. Krska, T. Kuiper-Goodman, M. Olsen, J. Pestka, S. Resnik, J. Schlatter, Deoxynivalenol. Safety Evaluation of Certain Mycotoxins in Food, in: WHO Food Addit. Ser. 47, 2001, pp. 420–555.
[2] J.C. Larsen, J. Hunt, I. Perrin, P. Ruckenbauer, Workshop on trichothecenes with a focus on DON: summary report, Toxicol. Lett. 153 (2004) 1–22.
[3] European Food Safety Authority, Deoxynivalenol in food and feed: occurrence and exposure, EFSA J. 11 (2013) 3379.
[4] T. Yoshinari, H. Takeuchi, K. Aoyama, M. Taniguchi, S. Hashiguchi, S. Kai, M. Ogiso, T. Sato, Y. Akiyama, M. Nakajima, S. Tabata, T. Tanaka, E. Ishikuro, Y. Sugita-Konishi, Occurrence of four *Fusarium* mycotoxins, deoxynivalenol, zearalenone, T-2 toxin, and HT-2 toxin, in wheat, barley, and Japanese retail food, J. Food Prot. 77 (2014) 1940–1946.
[5] P. Sobrova, V. Adam, A. Vasatkova, M. Beklova, L. Zeman, R. Kizek, Deoxynivalenol and its toxicity, Interdiscip. Toxicol. 3 (2010) 94–99.
[6] J.J. Pestka, A.T. Smolinski, Deoxynivalenol: toxicology and potential effects on humans, J. Toxicol. Environ. Health B Crit. Rev. 8 (2005) 39–69.
[7] M. Peraica, B. Radić, A. Lucić, M. Pavlović, Toxic effects of mycotoxins in humans, Bull. WHO 77 (1999) 754–766.
[8] FAO (Food and Agriculture Organization), Worldwide Regulations for Mycotoxins in Food and Feed in 2003, FAO Food and Nutrition Paper 81, FAO/UN, Rome, Italy, 2004.
[9] T. Tanaka, A. Yoneda, S. Inoue, Y. Sugiura, Y. Ueno, Simultaneous determination of trichothecene mycotoxins and zearalenone in cereals by gas chromatography-mass spectrometry, J. Chromatogr. A 882 (2000) 23–28.
[10] S.J. MacDonald, D. Chan, P. Brereton, A. Damant, R. Wood, Determination of deoxynivalenol in cereals and cereal products by immunoaffinity column cleanup with liquid chromatography: interlaboratory study, J. AOAC Int. 88 (2005) 1197–1204.
[11] K. Aoyama, H. Akashi, N. Mochizuki, Y. Ito, T. Miyashita, S. Lee, M. Ogiso, M. Maeda, S. Kai, H. Tanaka, H. Noriduki, H. Hiraoka, T. Tanaka, E. Ishikuro, Y. Itoh, T. Nagayama, M. Nakajima, S. Naito, Y. Sugita-Konishi, Interlaboratory study of LC-UV and LC-MS methods for the simultaneous determination of deoxynivalenol and nivalenol in wheat, Shokuhin Eiseigaku Zasshi 53 (2012) 152–156.
[12] T. Yoshinari, T. Tanaka, E. Ishikuro, M. Horie, T. Nagayama, M. Nakajima, S. Naito, T. Ohnishi, Y. Sugita-Konishi, Inter-laboratory study of an LC-MS/MS method for simultaneous determination of deoxynivalenol and its acetylated derivatives, 3-acetyl-deoxynivalenol and 15-acetyl-deoxynivalenol in wheat, Shokuhin Eiseigaku Zasshi 54 (2013) 75–82.
[13] Y. Sugita-Konishi, T. Tanaka, S. Tabata, M. Nakajima, M. Nouno, Y. Nakaie, T. Chonan, M. Aoyagi, N. Kibune, K. Mizuno, E. Ishikuro, N. Kanamaru, M. Minamisawa, N. Aita, M. Kushiro, K. Tanaka, K. Takatori, Validation of an HPLC analytical method coupled to a multifunctional clean-up column for the determination of deoxynivalenol, Mycopathologia 161 (2006) 239–243.
[14] A.Y. Kolosova, L. Sibanda, F. Dumoulin, J. Lewis, E. Duveiller, C. Van Peteghem, S. De Saeger, Lateral-flow colloidal gold-based immunoassay for the rapid detection of deoxynivalenol with two indicator ranges, Anal. Chim. Acta 616 (2008) 235–244.
[15] A.L. Albert, P.D. Champoux, A.H. Davis, QuickTox kit for QuickScan DON (vomitoxin), J. AOAC Int. 96 (2013) 1006–1016.
[16] Z. Dzuman, M. Vaclavikova, I. Polisenska, Z. Veprikova, M. Fenclova, M. Zachariasova, J. Hajslova, Enzyme-linked immunosorbent assay in analysis of deoxynivalenol: investigation of the impact of sample matrix on results accuracy, Anal. Bioanal. Chem. 406 (2014) 505–514.
[17] A. Lupo, C. Roebuck, K. Settimo, A. Quain, J. Kennedy, M. Abouzied, Validation study of a rapid ELISA for detection of deoxynivalenol in wheat, barley, malted barley, corn, oats, and rice, performance tested method 090901, J. AOAC Int. 93 (2010) 600–610.
[18] T. Kadota, Y. Takezawa, S. Hirano, O. Tajima, C.M. Maragos, T. Nakajima, T. Tanaka, Y. Kamata, Y. Sugita-Konishi, Rapid detection of nivalenol and deoxynivalenol in wheat using surface plasmon resonance immunoassay, Anal. Chim. Acta 673 (2010) 173–178.
[19] C. Maragos, Fluorescence polarization immunoassay of mycotoxins: a review, Toxins 1 (2009) 196–207.
[20] R. Abe, H. Ohashi, I. Iijima, M. Ihara, H. Takagi, T. Hohsaka, H. Ueda, "Quenchbodies": quench-based antibody probes that show antigen-dependent fluorescence, J. Am. Chem. Soc. 133 (2011) 17386–17394.
[21] R. Abe, H.J. Jeong, D. Arakawa, J. Dong, H. Ohashi, R. Kaigome, F. Saiki, K. Yamane, H. Takagi, H. Ueda, Ultra Q-bodies: quench-based antibody probes that utilize dye-dye interactions with enhanced antigen-dependent fluorescence, Sci. Rep. 4 (2014) 4640.
[22] H. Ueda, J. Dong, From fluorescence polarization to Quenchbody: recent progress in fluorescent reagentless biosensors based on antibody and other binding proteins, Biochim. Biophys. Acta 1844 (2014) 1951–1959.
[23] C.M. Maragos, L. Li, D. Chen, Production and characterization of a single chain variable fragment (scFv) against the mycotoxin deoxynivalenol, Food Agric. Immunol. 23 (2012) 51–67.
[24] T. Yoshinari, S. Sakuda, K. Furihata, H. Furusawa, T. Ohnishi, Y. Sugita-Konishi, N. Ishizaki, J. Terajima, Structural determination of a nivalenol glucoside and development of an analytical method for the simultaneous determination of nivalenol and deoxynivalenol, and their glucosides, in wheat, J. Agric. Food Chem. 62 (2014) 1174–1180.

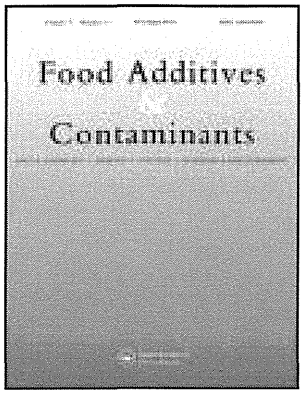

Food Additives & Contaminants: Part A
Publication details, including instructions for authors and subscription information:
http://www.tandfonline.com/loi/tfac20

Utility of the phylotoxigenic relationships among trichothecene-producing Fusarium species for predicting their mycotoxin-producing potential

M. Watanabe [a] , T. Yonezawa [b] , Y. Sugita-Konishi [a] & Y. Kamata [a]
[a] Division of Microbiology , National Institute of Health Sciences , Tokyo , Japan
[b] School of Life Sciences , Fudan University , Shanghai , China
Accepted author version posted online: 19 Apr 2013.Published online: 03 Jun 2013.

To cite this article: M. Watanabe , T. Yonezawa , Y. Sugita-Konishi & Y. Kamata (2013) Utility of the phylotoxigenic relationships among trichothecene-producing Fusarium species for predicting their mycotoxin-producing potential, Food Additives & Contaminants: Part A, 30:8, 1370-1381, DOI: 10.1080/19440049.2013.794305

To link to this article: http://dx.doi.org/10.1080/19440049.2013.794305

Food Additives & Contaminants: Part A, 2013
Vol. 30, No. 8, 1370–1381, http://dx.doi.org/10.1080/19440049.2013.794305

Taylor & Francis
Taylor & Francis Group

Utility of the phylotoxigenic relationships among trichothecene-producing *Fusarium* species for predicting their mycotoxin-producing potential

M. Watanabe[a]*, T. Yonezawa[b], Y. Sugita-Konishi[a] and Y. Kamata[a]

[a]*Division of Microbiology, National Institute of Health Sciences, Tokyo, Japan;* [b]*School of Life Sciences, Fudan University, Shanghai, China*

(*Received 1 May 2012; final version received 1 April 2013*)

Species of the genus *Fusarium* are well-known plant pathogens and mycotoxigenic fusaria are associated with health hazards to humans and animals. There is a need to understand the mechanisms of mycotoxin production by *Fusarium* species and to predict which produce mycotoxins. In this study, the *Fusarium* phylogenetic tree was first inferred among trichothecene producers and related species. We reconstructed the maximum likelihood (ML) tree based on the combined data from nucleotide sequences of rDNA cluster regions, the β-tubulin gene (*β-tub*) and the elongation factor 1α gene (*EF-1α*). Second, based on this tree topology, the ancestral states of the producing potential of type A and B trichothecenes (TriA and TriB), zearalenone (ZEN), moniliformin (MON), beauvericin (BEA) and enniatins (ENN) were reconstructed using the maximum parsimony (MP) method based on the observed production by extant species as reported in the literature. Finally, the species having the potential to produce each of these six mycotoxins was predicted on the basis of the parsimonious analysis. The ML tree indicated that the *Fusarium* species analysed in this study could be divided into two major clades. Clade I was divided into four distinct subclades: I-a, I-b, I-c and I-d. Furthermore, the parsimony reconstruction suggested that the potential for producing MON and ZEN was gained or lost only once, and that the producing potential for TriA and TriB, BEA and ENN was repeatedly gained and lost during the evolutionary history of the *Fusarium* species analysed in this study. Interestingly, the results showed the possibility that several species, about which reports were scarce with regard to mycotoxin production, have the potential to produce one or more of the six evaluated in this study. The phylogenetic information therefore helps one to predict the mycotoxin-producing potential by *Fusarium* species, and these "phylotoxigenic relationships" may be useful for predicting the pathogenicity of fungi.

Keywords: *Fusarium*; phylotoxigenic relationship; mycotoxin production; trichothecene; zearalenone; moniliformin; beauvericin; enniatin

Introduction

Species of the genus *Fusarium* are well-known, important plant pathogens, are mycotoxin producers, and are associated with human and animal health hazards (Marasas et al. 1984; Pitt & Hocking 2009). The *Fusarium* species produce several kinds of mycotoxins including trichothecenes, zearalenones (ZEN), moniliformin (MON), beauvericin (BEA) and enniatins (ENN) (e.g. Marasas et al. 1984; Yli-Mattila 2010). Trichothecenes elicit a range of toxic effects and some trichothecenes have been associated with deadly food-borne intoxications (Pitt & Hocking 2009). More than 70 trichothecenes have been identified and are classified into six categories, designated A–F based on their chemical structure, with type A and B trichothecenes (TriA and TriB) being among the most toxic. Therefore, there is a need to understand the mechanisms governing the production of trichothecenes by *Fusarium* species, and to predict which can produce these mycotoxins.

To solve these problems, it is necessary to infer a reliable species tree of trichothecene producers. Such a phylogenetic tree provides a platform for comparative studies about genetic and other states. Because characteristics are transferred to progeny genealogically, the evolutionary history of the trichothecene-producing potential of species within the *Fusarium* phylogenetic tree can be traced. Phylogeny can be regarded as a powerful tool for predicting the characteristics of living organisms as, for example, previous studies have found a correlation between phylogenetic lineages and the producing potential for particular mycotoxins (Knutsen et al. 2004; Kristensen et al. 2005).

One problem in the field of *Fusarium* research is the imprecise taxonomic system of the genus. The existing classification schemes for fungi are dominantly based on their morphological characteristics (Taylor et al. 2000). Although traditional taxonomic systems for the genus *Fusarium* have also been proposed based on the morphological states, the taxonomy of this genus has been debated for many years (Wollenweber & Reinking 1935; Booth 1971; Joffe 1974; Gerlach & Nirenberg 1982; Nelson et al. 1983). Recently, researchers have applied molecular phylogenetic analyses to the taxonomy of *Fusarium* species (e.g. Seifert & Levesque 2004;

*Corresponding author. Email: mwatanabe@nihs.go.jp

O'Donnell et al. 2007, 2010; Gilmore et al. 2009; Grafenhan et al. 2011). Some phylogenetic relationships remain unclear, however, because many molecular–phylogenetic analyses for a particular lower taxonomic group have been narrowly focused and some phylogenetic trees have had low resolution due to the lack of suitable nucleotide and amino acid substitution rates. Watanabe et al. (2011) and Kristensen et al. (2005) reported the comprehensive phylogenetic tree of the entire *Fusarium* species and trichothecene producers and its related species, respectively, and were able to show some new phylogenetic relationships. However, their studies did not sufficiently elucidate the evolutionary history of the trichothecene producers because their dataset did not include a sufficient number of species.

In this study, the *Fusarium* phylogenetic tree was inferred among trichothecene producers and related species. Furthermore, the ancestral states of trichothecene production capacity were reconstructed based on this tree topology, and the producing potential of extant species was predicted.

Materials and methods

Strains

The strains used in this study are listed in Table 1. We selected 14 species or subspecies from the genus *Fusarium*. To select these species, we referred to the nomenclature system proposed by Nelson et al. (1983), which is a very simple and systematic morphological taxonomy that is

Table 1. Strains of the genus *Fusarium* and *Fusarium*-related species used in this study.

Section[a]	Species registered by resource organisation	Species in the traditional taxonomic system	Strain number
Arthrosporiella	*F. incarnatum*	*F. semitectum*	MAFF[b] 236521
			MAFF 236386
	F. camptoceras	*F. camptoceras*	CBS[c] 193.65
Discolour	*F. culmorum*	*F. culmorum*	MAFF 236454
			IFM[d] 50210
	F. cerealis	*F. crookwellense*	MAFF 241212
			MAFF 101144
	F. crookwellense		NBRC[e] 32585
	F. asiaticum	*F. graminearum*	MAFF 240264
	F. graminearum		MAFF 240270
Gibbosum	*F. equiseti*	*F. equiseti*	MAFF 236434
			MAFF 236723
	F. longipes	*F. longipes*	IFM 50036
	F. scirpi	*F. scirpi*	CBS 448.84
	F. acuminatum subsp. *armeniacum*	*F. acuminatum*	CBS 485.94
			MAFF 236716
	F. acuminatum subsp. *acuminatum*		NZ 50
			ICMP10524Q
Lateritium	*F. lateritium*	*F. lateritium*	MAFF 235344
			MAFF 840045
Roseum	*F. avenaceum*	*F. avenaceum*	ATCC[f] 200255 (type)
			MAFF 239206
Sporotrichiella	*F. kyushuense*	Not described	MAFF 237645 (ex-holotype)
			NRRL[g] 6490 (type)
	F. langsethiae	Not described	CBS 113234 (holotype)
			FRC[h] T-1000
	F. poae	*F. poae*	FRC T-0796
			MAFF 305947
	F. sporotrichioides	*F. sporotrichioides*	ATCC 34914
			CBS 119839
	Gibberella tricincta	*F. tricinctum*	ATCC 38183 (type)
	F. tricinctum		CBS 393.93 (epitype)

Notes: [a]Nelson et al. (1983).
[b]Ministry of Agriculture, Forestry and Fisheries.
[c]Centraalbureau voor Schimmelcultures.
[d]Medical Mycology Research Center, Chiba University.
[e]National Institute of Technology and Evaluation, Biological Resource Center.
[f]American Type Culture Collection.
[g]Agricultural Research Service Culture Collection of the US Department of Agriculture.
[h]*Fusarium* Research Center, Pennsylvania State University.

widely applied in the field to identify *Fusarium* isolates. To cover a wider range of taxonomic groups, we selected two additional species referring to morphological, molecular phylogenetic and mycotoxin profile studies (Aoki & O'Donnell 1998; Knutsen et al. 2004; Thrane et al. 2004; Torp & Nirenberg 2004), and two subspecies, namely *F. acuminatum* subsp. *armeniacum* and subsp. *acuminatum* (Table 1). Between these subspecies there is a large genetic distance, a distant phylogenetic relationship and different states of mycotoxin production. This analysis tested a total of 32 strains including one to three strains for each species or subspecies examined.

DNA extraction and sequence determination of genes

In this study, nucleotide sequences of genes of eight strains were determined: MAFF 236386, CBS 193.65, MAFF 236454, IFM 50210, MAFF 101144, NBRC 32585, IFM 50036 and CBS 448.84. We used two subcultures of each of eight *Fusarium* species obtained by the single spore method (Nelson et al. 1983) for sequencing. We checked the sequence identity between two subcultures to confirm the purity of the strain. Incubation of the fusaria and extraction of genomic DNAs from these samples were performed as previously described (Watanabe et al. 2011).

The ribosomal RNA gene (rDNA) cluster region, including the 3′ end of the 18S rDNA, the internal transcribed spacer region 1 (ITS1), the 5.8S rDNA and the 5′ end of the 28S rDNA, as well as the β-tubulin gene (*β-tub*) and the elongation factor 1α gene (*EF-1α*), were analysed. These regions were selected because some parts of the rDNA cluster region, *β-tub* and *EF-1α* have previously been used as genetic markers for the phylogenetic analysis of fungal taxonomic groups, including *Fusarium* species (O'Donnell 1993; O'Donnell et al. 1998; Watanabe et al. 2011). These genes were amplified and sequenced with the primer pairs as previously described (Watanabe et al. 2011). The sequences were assembled using the ATGC software program (Genetyx Corporation, Tokyo, Japan). The sequences determined in this study were deposited in GenBank (Accession Nos AB820701–AB820724).

Downloaded sequences of genes from earlier studies

Nucleotide sequences of the genes of 24 strains (which do not include the eight strains listed in Table 1) that were determined in previous studies (Harrow et al. 2010; Watanabe et al. 2011) were downloaded from GenBank (Accession Nos AB586983, AB586988-586992, AB586 999-05, AB587015, AB587016, AB587019-587021, AB 587024-587026, AB587036, AB587038-587040, AB587 047-587053, AB587063, AB587064, AB587067-587069, AB587072-587078, AB674263, AB674264, AB674267-674270, AB674277-674282, AB674292, AB674293, AB674296-AB674298, AB674301-674304, EU008509, EU008531, EU490248 and EU490226).

Alignment

Sequences were automatically aligned by the MAFFT software program, v.6 (Katoh et al. 2009) with the G-INS-i option, and were also carefully checked by

Table 2. Mycotoxin production of the extant species based on the literature.

Species	Clade number in Figure 1	Mycotoxin					
		Tri-A	Tri-B	ZEN	MON	BEA	ENN
F. graminearum s.l.	I-a	1[a]	1	1	0[b]	0	0
F. crookwellense		0	1	1	?[c]	0	0
F. culmorum		0	1	1	1	0	0
F. poae	I-b	1	1	1	?	1	1
F. kyushuense		0	1	?	?	0	1
F. langsethiae	I-c	1	0	?	?	1	1
F. sporotrichioides		1	0	1	1	1	1
F. acuminatum subsp. *armeniacum*		1	?	?	?	?	?
F. scirpi	I-d	?	?	?	?	?	1
F. equiseti		1	1	1	1	1	0
F. longipes		?	?	?	?	1	?
F. semitectum		1	0	1	1	1	?
F. camptoceras		?	?	?	?	?	?
F. tricinctum	II	0	0	?	1	?	1
F. lateritium		0	0	0	?	?	1
F. avenaceum		0	0	0	1	1	1
F. acuminatum subsp. *acuminatum*		1	?	?	?	?	?

Notes: [a]This species has the potential for mycotoxin production.
[b]This species does not have the potential for mycotoxin production.
[c]This species may or may not produce mycotoxin, regarded as missing data.

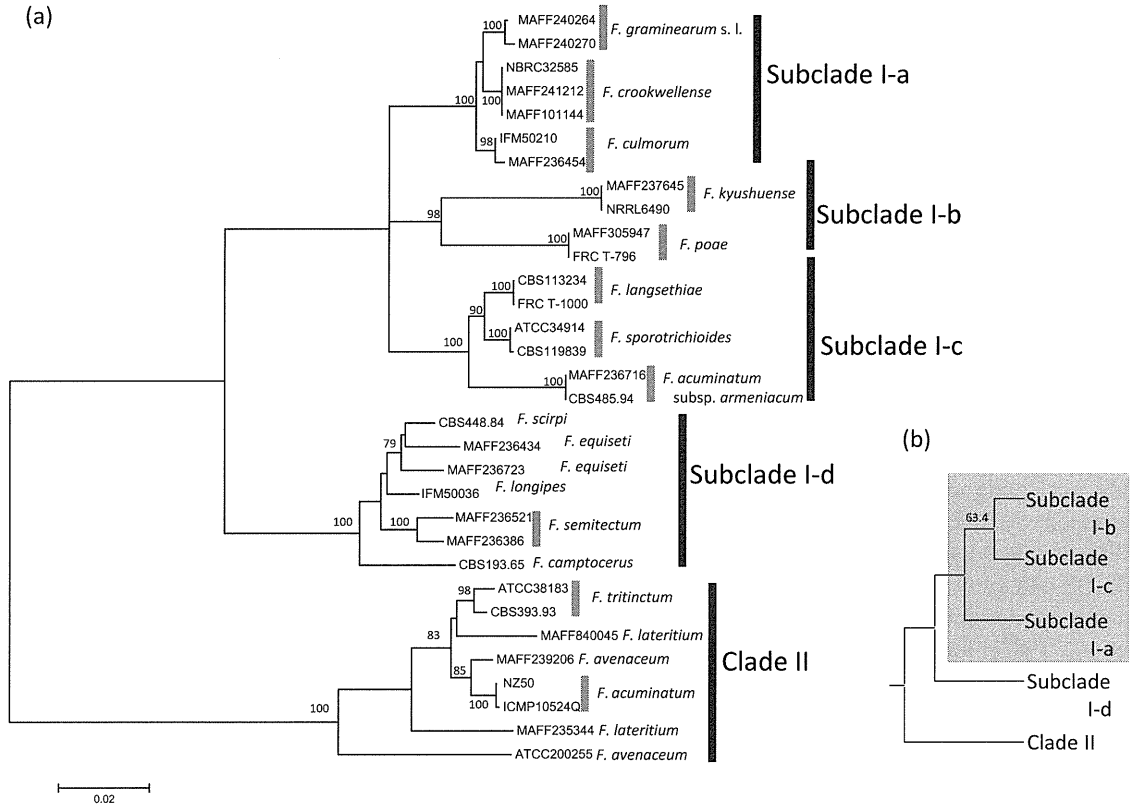

Figure 1. (a) Maximum likelihood tree as inferred from the combined nucleotide sequence data of three independent genetic regions: the rDNA cluster, *EF-1α* and *β-tub*. Tree topology was inferred by the RAxML program using the GTR + I + Γ model with the partition. Nodal numbers indicate bootstrap probabilities (1000 replications). Branch lengths were re-estimated by using a more realistic model (CS + Γ model for exon regions, GTR + Γ model for introns and the rDNA cluster, with the PAML package). Nodes that were supported at a 50% bootstrap probability level or lower were treated as multifurcations. Branch lengths are proportional to the numbers of nucleotide substitutions per nucleotide site. Numbers of codon substitutions per codon sites were recalculated based on the numbers of codon substitutions per nucleotide site. The relationships among five clades were fixed, referring to the ML tree in Watanabe et al. (2011), because these basal relationships are very important for the ancestral state reconstructions of mycotoxin productivities. (b) Phylogenetic relationships among the subclades in clade I. The CS + Γ model and GTR + Γ model were applied by using the PAML. Nodal number indicates the RELL bootstrap value (100, 000 replications) determined using the CONSEL program.

visual inspection. All ambiguous sites of alignment were excluded from the analyses. The final sequence lengths of each gene locus were as follows: rDNA (801 bp; ITS1 was 109 bp, 5.8S rRNA was 159 bp, 28S rRNA was 533 bp), *EF-1α* (597 bp; exons were 201 bp and introns were 376 bp), and *β-tub* (871 bp; exons were 786 bp and introns were 85 bp).

Phylogenetic inference

The phylogenetic tree was inferred by the maximum likelihood (ML) method (Felsenstein 1981). The data consisted of the exon regions (*EF-1α*, *β-tub*), intron regions (*EF-1α*, *β-tub*), an internal spacer region of rDNA (ITS1), and rDNA regions (5.8S, 28S) of the selected genes. The tempo and modes of the nucleotide substitutions for these regions are very different, and the codon substitution (CS; Yang et al. 1998) model is suitable for a reconstruction of a "true" tree even with these differences, because the evolutionary unit of the CS model is a codon site. This model takes into account the differences in the physicochemical distance between the amino acids and the ratios of synonymous and non-synonymous substitution rates, as well as the correlation of the three nucleotide sites included in the codon. Yonezawa et al. (2008) demonstrated that the support value of a "true" tree was increased by improvement of the model, and it became the highest when the CS mode was applied. However, computation using the CS model is time-, labour- and cost-intensive, and almost impossible to apply for tree searches from the huge numbers of candidate trees. Therefore, a heuristic search using a simple model was first carried out to reduce the number of candidate trees. An exhaustive search using the CS model was then carried out after the candidate tree topologies had been narrowed down.

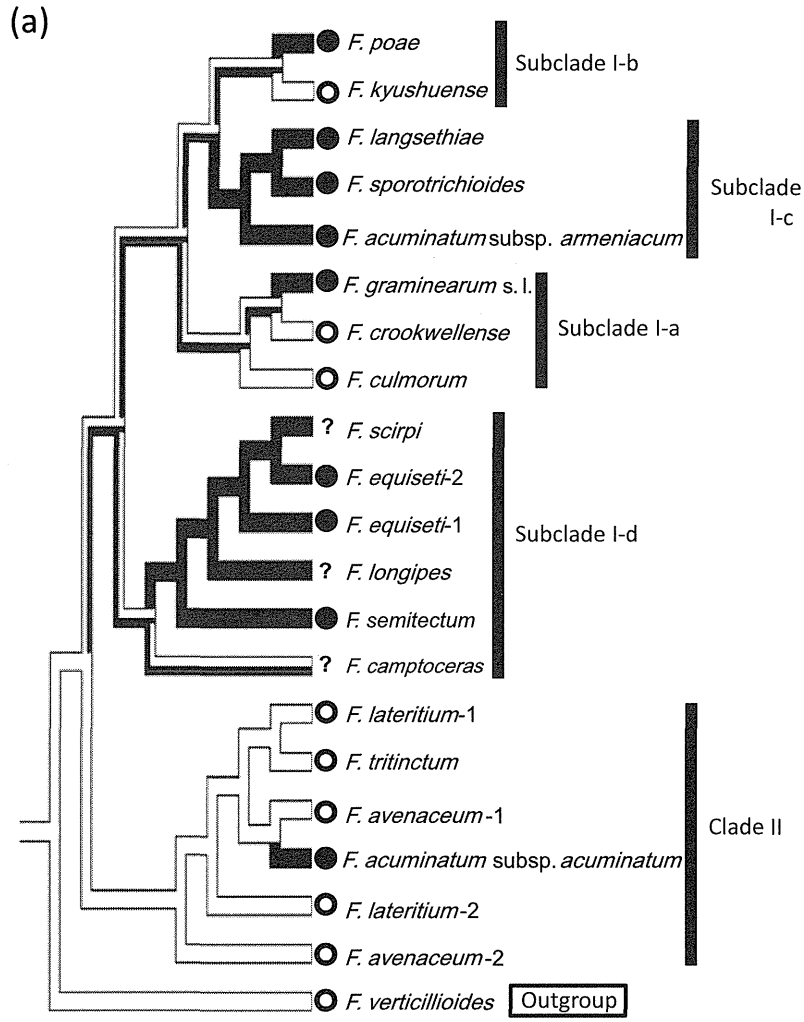

Figure 2. Ancestral state reconstruction of the mycotoxin-producing potential production: (a) type A trichothecene; (b) type B trichothecene; (c) zearalenone; (d) moniliformin; (e) beauvericin; and (f) enniatins. The ancestral states of the internal nodes were reconstructed based on the character states of the production of the extant *Fusarium* species, profiled based on the literature. The ancestral states were reconstructed by the MP method using the MESQUITE program v.2.75 (see http://mesquiteproject.org/mesquite/mesquite.html) on the tree topology inferred in this study (Figure 1). The white branch means the absence of the toxic productivity. The black branch means the presence of the toxic productivity, estimated by the ancestral state reconstruction. The black and white branch means both the absence and the presence equally supported by the parsimonious criterion. The character state of a species from the literature is indicated beside the terminal branch; the open circle means the absence of the toxic productivity; the filled circle means the presence of the toxic productivity; and the question mark means the states of the production is unclear in the literature.

The heuristic search was carried out by using the RAxML program, v.7.2.6 (Stamatakis et al. 2008). The confidence levels of the internal nodes were evaluated by the rapid bootstrap (BP) method (Stamatakis et al. 2008) with 1000 replications. The GTR + I + Γ model (Hasegawa et al. 1985; Yang 1996) was used as the nucleotide substitution model. Watanabe et al. (2011) demonstrated that the tempo and mode of the nucleotide substitutions in each locus used as a genetic marker for *Fusarium* phylogeny in that study were variable. Taking into account such differences among loci, the partition model (Pupko et al. 2002) was applied. The fitting of the partitioning to the respective gene loci was evaluated by the Akaike information criterion (AIC; Akaike 1973) to avoid over-parameterisation (data not shown). Eight partitions were set for the concatenated data as follows: ITS1, 5.8S rRNA + 28S rRNA, first and second codon positions of *EF-1α*, third codon positions in the exon of *EF-1α*, introns of *EF-1α*, first codon position of *β-tub*, second codon position of *β-tub*, third codon position of *β-tub* and introns of *β-tub*.

An exhaustive search was carried out using both the BASEML and CODEML programs in PAML v.4.4 (Yang 2007). The GTR + Γ model (Yang 1996) was applied for

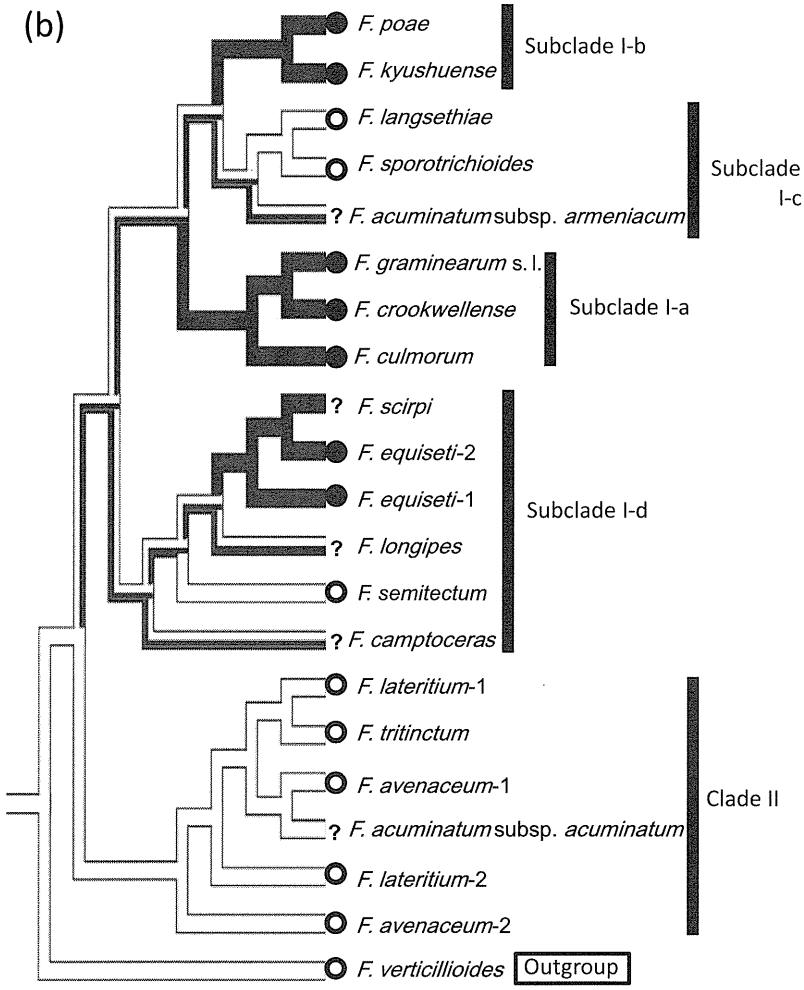

Figure 2. Continued.

the non-coding regions; the CS + Γ model (Yang et al. 1998) was applied for the exon regions. The amino acid distances were then estimated (Miyata et al. 1979). In this analysis we also evaluated the partitioning by AIC using the information obtained from this exhaustive search. Five partitions were set for the concatenated data as follows: rDNA cluster, exons of *EF-1α*, introns of *EF-1α*, exons of *β-tub* and introns of *β-tub*. The branch lengths for each partition were independently estimated. The CONSEL program (Shimodaira & Hasegawa 2001) was applied for summing up the likelihood score for each gene locus; the SH test (Shimodaira & Hasegawa 1999) was applied to evaluate the differences among tree topologies.

Profiling the mycotoxin production and ancestral state reconstruction

To trace the evolutionary history of mycotoxin-producing potential, the ancestral states of the internal nodes were reconstructed using the *Fusarium* tree topology inferred in this study (Figure 1). The production capacities of six mycotoxins, namely TriA, TriB, ZEN, MON, BEA and ENN, of the extant species were profiled based on the literature (Rabie et al. 1982; Marasas et al. 1984; Lee et al. 1986; Scott et al. 1987; Chelkowsk et al. 1990; Gupta et al. 1990; Bosch & Mirocha 1992; Wing et al. 1993; Herrman et al. 1996; Logrieco et al. 1998; Turner et al. 1998; Logrieco et al. 2002; Nicholson et al. 2004; Thrane et al. 2004; Leslie et al. 2006; Yli-Mattila 2010). In this procedure, a species was regarded as having the potential to be a mycotoxin producer when two or more strains have been reported to produce it. If no literature was available on the mycotoxin-production capability of a species, this was regarded as missing data. The constructed character state matrix is shown in Table 2.

Because we confirmed that the MP method is reliable for the ancestral state reconstruction of the mycotoxin production, in addition to the ML method (see Supplementary Text 2, available via the article webpage), the ancestral states were

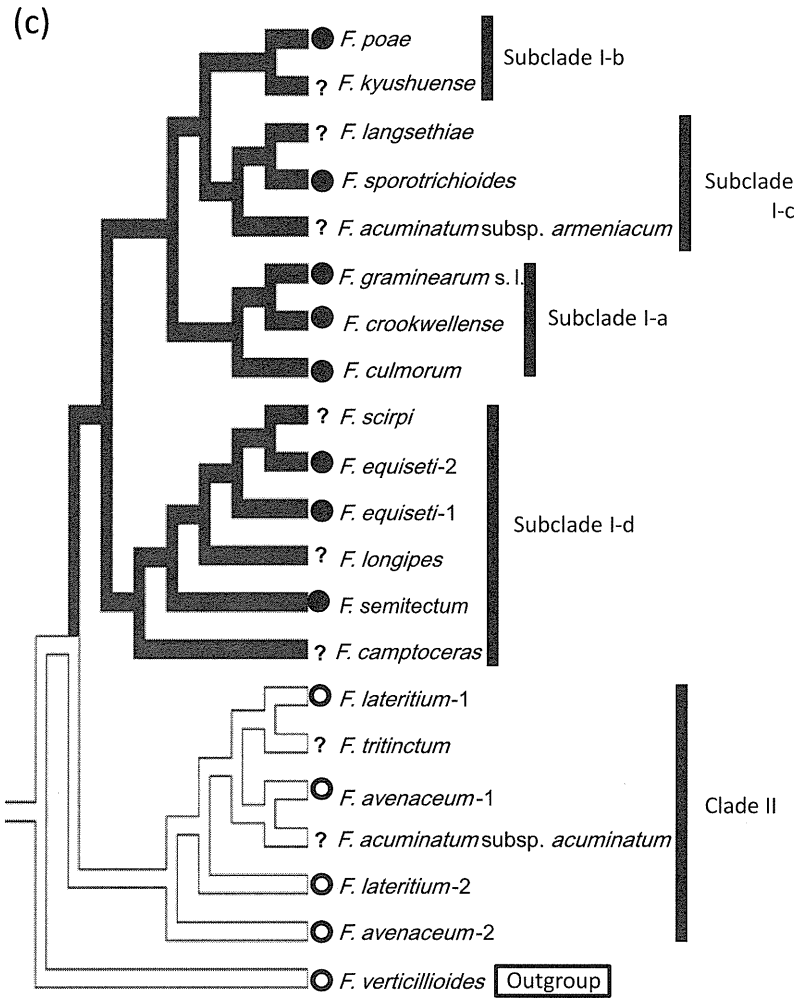

Figure 2. Continued.

reconstructed by the MP method (Pagel 1999) using the MESQUITE program v.2.75 (see http://mesquiteproject.org/mesquite/mesquite.html). The topology of the *Fusarium* tree of the combined sequences of the three genetic regions was provided from the results of the ML tree used in this study.

Results and discussion

There are four major groups of the trichothecene species

In this study we used three independent gene loci as genetic markers. Inconsistencies among gene trees have often been reported (Nishihara et al. 2009; Watanabe et al. 2011). It is therefore necessary to confirm that there are no inconsistencies among the gene trees and, in this study, we evaluated the conflict among the tree topologies supported by each gene (see Supplementary Text 1). Because no statistically significant differences were found, we inferred that the ML tree, which was constructed based on the combined sequence data for the three genetic regions, could be used: the rDNA cluster, *β-tub* and *EF-1α*. The results are shown in Figure 1(a). The *Fusarium* species analysed in this study were divided into two major clades, I and II, a result strongly supported by a 100% BP. This result was consistent with a previous study (Watanabe et al. 2011).

Furthermore, clade I was divided into four distinct subclades, I-a to I-d, which corresponded to four previously reported clades (Kristensen et al. 2005). Subclade I-a consists of *F. crookwellense*, *F. graminearum sensu lato* (s.l.), and *F. culmorum*. Subclade I-b consists of *F. kyshuense* and *F. poae*, while subclade I-c consists of *F. langsethiae, F. sporotrichioides* and *F. acuminatum* subsp. *armeniacum*. Subclade I-d consists of *F. camptoceras*, *F. semitectum*, *F. longipes*, *F. equiseti* and *F. scirpi*. Clade II includes the remaining species.

Within clade I, the basal position of subclade I-d was strongly supported with a 100% BP. Furthermore, the monophyly of subclades I-a and I-b was weakly supported

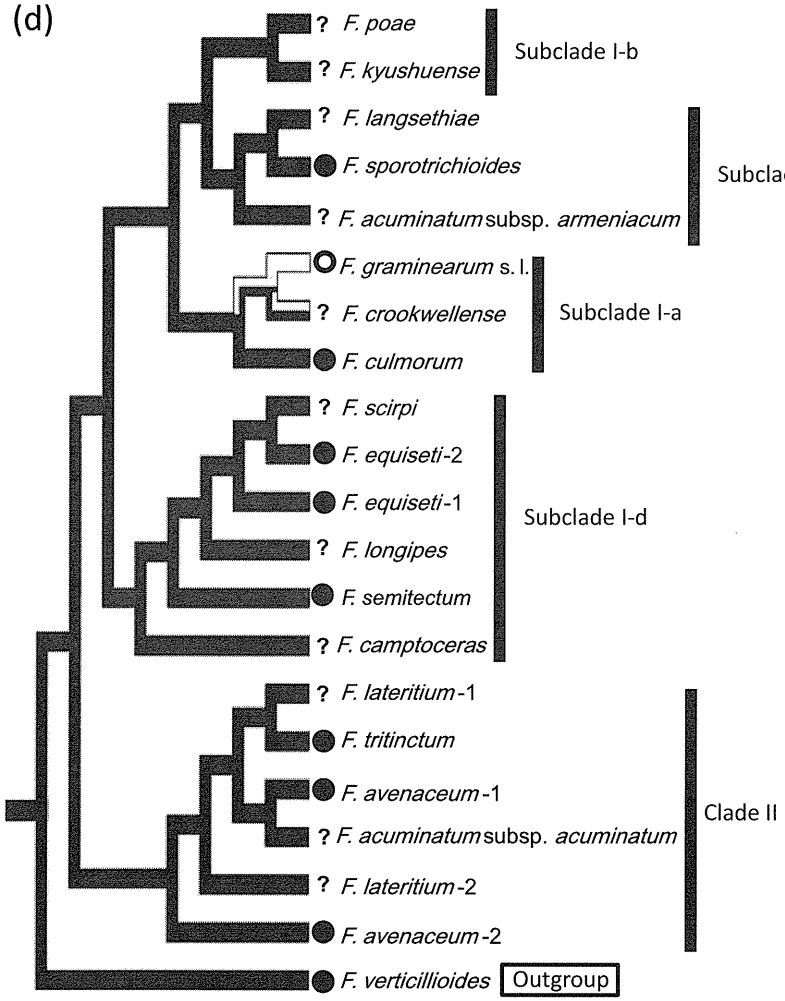

Figure 2. Continued.

with a 46% BP (in Figure 1(a), subclades I-a, I-b and I-c formed a polyphyletic clade). Since the monophyly of subclades I-b and I-c has been suggested by both morphological (Booth 1971; Nelson et al. 1983) and molecular (Kristensen et al. 2005) studies, we carried out a more detailed comparison of relationships among subclades I-a, I-b and I-c using the CS substitution model (see the "Materials and methods" section).

The ML tree inferred from this further analysis (see Supplementary Table 5) is shown in Figure 1(b). The monophyly of subclades I-b and I-c was consistent with the previous morphological and molecular studies mentioned above, although this clade was weakly supported with a 63.4% BP in the analysis. Therefore, we assumed that there was a monophyletic relationship between subclades I-b and I-c, and this topology was used in the reconstruction of the ancestral states of the mycotoxin production in this study.

Ancestral states of mycotoxin-producing potential

We estimated the ancestral states of the mycotoxin-producing potential by the MP method (see Supplementary Text 2) using the dataset of the mycotoxin production of the extant species based on the literature (Table 2). The results showed the possibility that the common ancestor of all tested species in this study had the potential to produce MON, BEA and ENN (Figures 2(d), (e) and (f)). In a parsimonious manner, the potential to produce MON and ZEN was gained or lost only once in the evolutionary history of the *Fusarium* species analysed in this study. The common ancestor of the clade I gained the ZEN-producing potential (Figure 2(d)). The common ancestor of *F. graminearum* s.l. or one of *F. graminearum* s.l./*F. crookwellense* lost the MON-producing potential only once (Figure 2(c)). These results suggest that the structures responsible for the ZEN and MON-producing potential had a lower incidence of

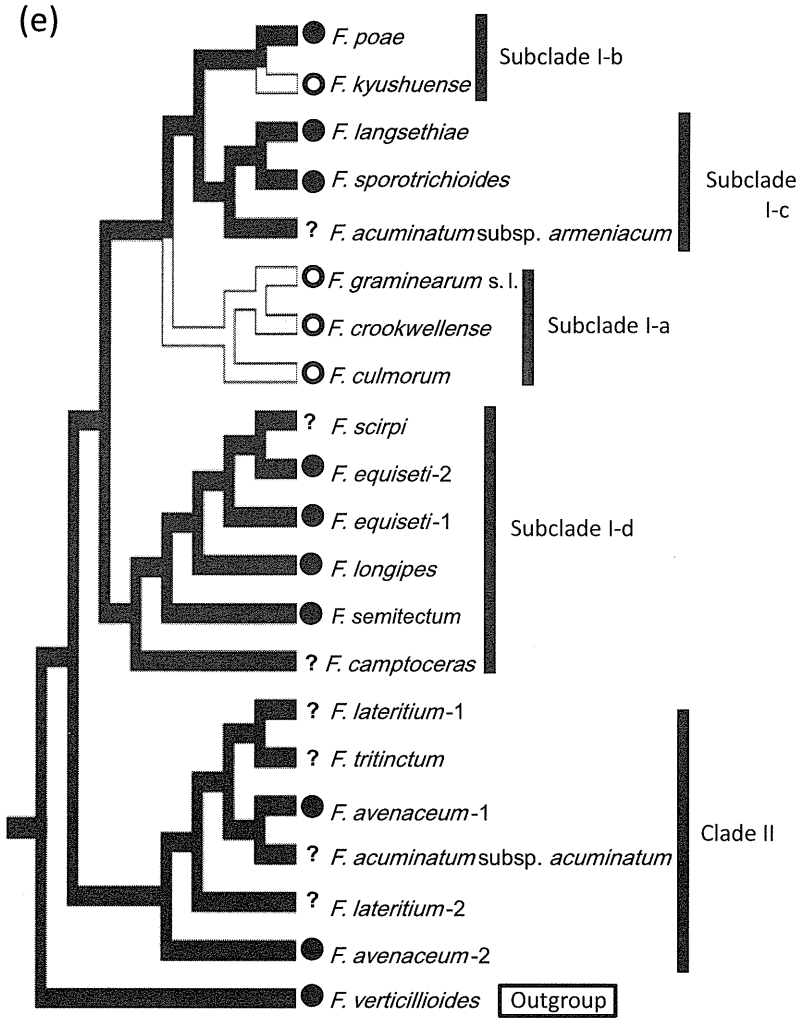

Figure 2. Continued.

changes, and it is thought that this structure was stable during the evolution of *Fusarium* species. On the other hand, the potential to produce TriA, TriB, BEA or ENN was independently gained or lost repeatedly. In the case of TriA, TriB, BEA or ENN, the producing potential was gained or lost four times, three times, twice and three times, respectively, in the evolutionary history of clade I (Figures 2(a), (b), (e) and (f)). The TriA-producing potential was gained one more time in the common ancestor of *F. acuminantum* subsp. *acuminatum* in clade II. In the case of the BEA-producing potential, *F. kyushuense* and the common ancestor of subclade I-a gained the producing potential (Figure 2(e)). Our parsimony reconstruction showed that the TriA-producing potential had the most frequent events of gain or loss among the six mycotoxins analysed. This suggested that the structure responsible for the production of TriA, such as the biosynthetic gene cluster (Desjardins & Proctor 2007), was comparably easy to change, thus resulting in a loss or gain of function.

In the case of the TriA- and TriB-producing potential, the parsimony reconstruction indicated that there are different trends between clade I which underwent many changes and clade II which did not (Figures 2(a) and (b)). Based on these results, it is possible that the species in clade II have a factor that prevents changes in the structure responsible for producing these mycotoxins. Therefore, we can presume that the ease by which mycotoxin-production changes in these two clades may have varied throughout the history of *Fusarium* evolution.

The genes encoding the enzymes involved in the biosynthesis systems for many mycotoxins have been identified and found to form gene clusters. In addition, other genes are involved in mycotoxin production and include transcriptional regulators, transporters and others. Because the genes in the cluster should be co-expressed when

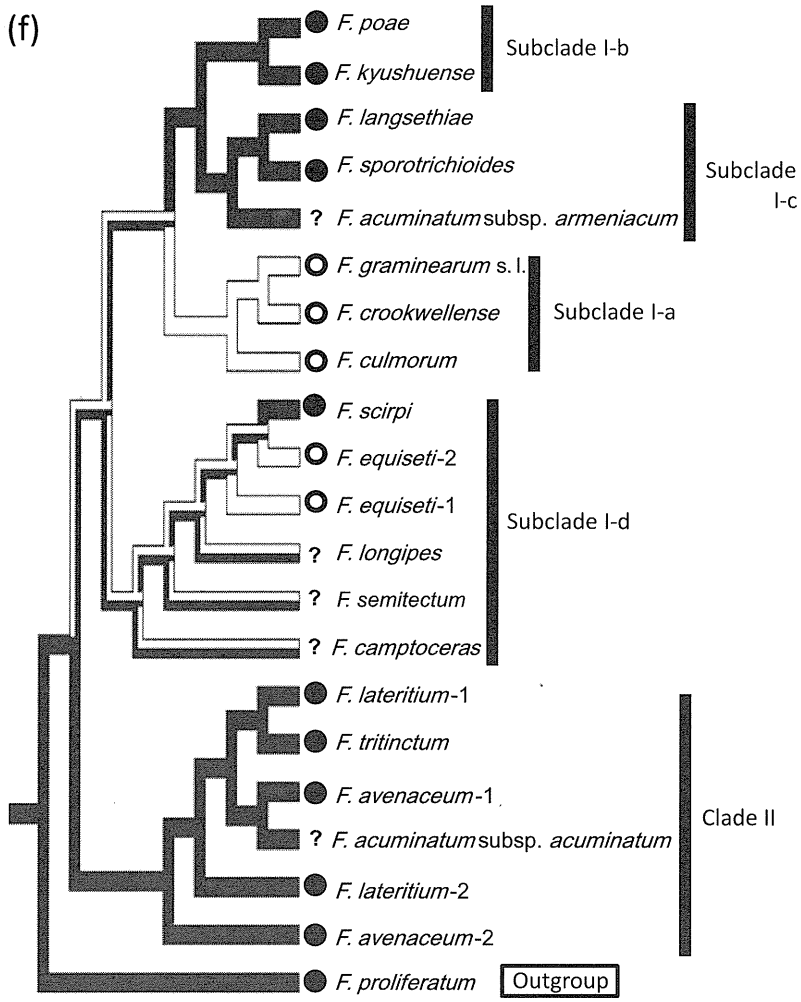

Figure 2. Continued.

mycotoxin is produced, the genome requires that all or almost all genes in the cluster have a role in mycotoxin production so that if the function of any gene(s) in a biosynthetic gene cluster is inhibited, the mycotoxin could not become produced. Previous studies revealed that some evolutionary factors have had an impact on gene function stability in fungal genomes. In other words, the evolutionary rate of mycotoxin-producing genes was accelerated or slowed by these factors. For example, the adaptive evolution involved in the biological role of mycotoxins was identified (Ward et al. 2002; Reverberi et al. 2010) and, furthermore, it has been suggested that a particular mycotoxin productivity was acquired by horizontal gene transfer (Khaldi & Wolfe 2011). These evolutionary events may be related to the frequency of gain/loss in productivities of the six mycotoxins analysed in this study via changes in the biosynthetic gene cluster. There remains a need for future investigations to reveal the evolutionary event(s) affecting *Fusarium* genomes and the variability in production of the six mycotoxins considered in this study.

Predicting mycotoxin production

We predicted mycotoxin production by *Fusarium* species (which had no literature reports for the six mycotoxins analysed in this study) based on the results shown in Figures 2(a)–(f). It is of interest that the results showed the possibility that some species, including *F. camptoceras*, *F. longipes and F. scirpi*, about which previous reports were scarce with regard to mycotoxin production, have the potential to produce some mycotoxins (Nelson et al. 1983; Marasas et al. 1984; Leslie et al. 2006). These three species are generally thought to have little to no toxicity, even though they are closely related to other species of subclade I-d that produce trichothecenes, ZEN, MON and BEA. The findings suggested that these "little or non-toxic species" may have the potential to